

# Homopolyatomic Anions and Configurational Questions. Synthesis and Structure of the Nonagermanide(2-) and Nonagermanide(4-) Ions, $\text{Ge}_9^{2-}$ and $\text{Ge}_9^{4-}$

Claude H. E. Belin, John D. Corbett,\* and Alan Cisar

Contribution from the Ames Laboratory-ERDA and Department of Chemistry, Iowa State University, Ames, Iowa 50011. Received March 31, 1977

**Abstract:** Reaction of solid KGe with 2,2,2-crypt (4,7,13,16,21,24-hexaoxa-1,10-diazobicyclo[8.8.8]hexacosane) in ethylenediamine yields deep-red rods which have been shown to be  $(\text{crypt-K}^+)_6\text{Ge}_9^{2-}\text{Ge}_9^{4-}\cdot 2.5\text{en}$  by x-ray crystallography. The compound crystallizes in the  $P\bar{1}$  space group with  $Z = 2$  and  $a = 20.037(2) \text{ \AA}$ ,  $b = 28.944(2) \text{ \AA}$ ,  $c = 14.546(2) \text{ \AA}$ ,  $\alpha = 99.356(8)^\circ$ ,  $\beta = 94.077(8)^\circ$ , and  $\gamma = 87.60(1)^\circ$ ,  $V = 8312.9(12) \text{ \AA}^3$  at  $25^\circ\text{C}$ . Diffraction data were measured over four octants using a four-circle automated diffractometer and monochromatized  $\text{Mo K}\alpha$  radiation, and the structure was solved by direct methods and Fourier techniques. The 190 independent (nonhydrogen) atoms in the structure yielded, with anisotropic thermal parameters for germanium and potassium,  $R = 0.149$  and  $R_w = 0.169$  for 8409 independent observed reflections with  $2\theta \leq 50^\circ$ . Charges on the two  $\text{Ge}_9$  cluster ions were assigned according to their relationship to the isoelectronic  $\text{Sn}_9^{4-}$  ( $C_{4v}$ ) and  $\text{B}_9\text{H}_9^{2-}$  ( $D_{3h}$ ). The  $\text{Ge}_9^{4-}$  ion configuration is quite close to the ideal  $C_{4v}$ ,<sup>2</sup> with a nearly square base (3.58 and 3.64  $\text{ \AA}$  diagonals and a vicinal dihedral angle  $\delta$  5.3 $^\circ$ ) and  $\delta$  162 and 156 $^\circ$  for the characteristic opposed faces parallel to the fourfold axis (158 $^\circ$  in  $\text{Sn}_9^{4-}$ ). The  $\text{Ge}_9^{2-}$  ion exhibits essentially  $C_{2v}$  symmetry but clearly derives from the  $D_{3h}$  limit, with 2.81, 2.86, and 3.17  $\text{ \AA}$  for the parallel edges of the trigonal prism,  $\delta$  171 $^\circ$  for the opposed faces therein, and capping atoms separated by 4.00, 4.16, and 4.22  $\text{ \AA}$ . Atomization energies from SCF-MO-CNDO calculations support the charge assignment deduced geometrically, the differentiation of configurations arising almost entirely from the  $\text{Ge}_9^{2-}$  ion. The observed distortion of this ion may relate to the generation of a small dipole moment. The configurational contrast between the highly polar  $\text{Sn}_9^{4-}$  and  $\text{Ge}_9^{4-}$  ( $C_{4v}$ ) and the isoelectronic but apolar  $\text{Bi}_9^{5+}$  ( $D_{3h}$ ) is considered further.

The extensive electrochemical studies of Zintl and co-workers<sup>3-6</sup> on solutions of alkali metal alloys of posttransition elements in liquid  $\text{NH}_3$  served to identify such homopolyatomic anions as  $\text{Pb}_9^{4-}$ ,  $\text{Pb}_7^{4-}$ ,  $\text{Sn}_9^{4-}$ ,  $\text{Sb}_3^{3-}$ ,  $\text{Sb}_7^{3-}$ , and  $\text{Bi}_5^{3-}$ . In general the evaporation of ammonia from these solutions gave either amorphous products or phases already known in the corresponding alloy systems, the species present in the ammonia solution being almost impossible to isolate in the crystalline state because of the greater stability of (electron delocalization in) the alloy systems. In a parallel manner some of the same condensed alloy systems exhibit intermetallic compounds with properties indicative of polar bonding (Zintl phases) and homopolyatomic species,<sup>7</sup> giving further incentive to the synthesis and investigation of compounds containing isolated examples of such polyatomic groups.

Recently a general route to the stabilization and thence isolation of some of the above and other homopolyatomic anions has been discovered, utilizing the bicyclic 2,2,2-crypt<sup>8</sup> to complex the sodium or potassium counterion and thus to prevent electron transfer back onto the cation in the solid state. This approach has now allowed the isolation and structural characterization of the stable polyanions  $\text{Sn}_9^{4-}$ ,<sup>2,9</sup>  $\text{Pb}_5^{2-}$  and  $\text{Sn}_5^{2-}$ ,<sup>10</sup>  $\text{Sb}_7^{3-}$ ,<sup>11,12</sup>  $\text{Te}_3^{2-}$ ,<sup>13</sup> and  $\text{Bi}_4^{2-}$ .<sup>14</sup>

In the particular case of germanium, Zintl and Kaiser<sup>6</sup> were able to generate a dilute brown solution by ammonia extraction of sodium-germanium alloys, but electrochemical attempts at the production of the germanium solutions were unsuccessful. Recently Diehl et al.<sup>15</sup> have reported that sodium-germanium alloys also dissolve very slowly in warm ethylenediamine (en) alone and that after some weeks copper-colored crystals of composition  $\text{Na}_4\text{Ge}_9\cdot 5\text{en}$  may be isolated. We have found that deep red, lavender, and copper colored phases can be readily isolated from reactions of sodium- or potassium-germanium phases with crypt in ethylenediamine. The present paper reports the structure of the first of these,  $(\text{crypt-K}^+)_6\text{Ge}_9^{2-}\text{Ge}_9^{4-}\cdot 2.5\text{en}$ . The  $\text{Ge}_9^{2-}$  found represents a new electronic structure for homopolyatomic ions whereas the  $\text{Ge}_9^{4-}$  is closely analogous to  $\text{Sn}_9^{4-}$  and a second example

of the novel uncapped square antiprismatic configuration ( $C_{4v}$ ).<sup>2</sup> Subsequent research has shown that the violet phase is evidently  $(\text{crypt-K}^+)_2\text{Ge}_9^{2-}$  but the copper compound is badly disordered on anion sites.<sup>16</sup>

## Experimental Section

**Synthesis.** The phase KGe was prepared by heating the stoichiometric amounts of the elements to  $700^\circ\text{C}$  in a tantalum tube which had previously been weld sealed in a helium atmosphere. The composition  $\text{KGe}_{1.8}$  was subsequently prepared by reaction of finely powdered KGe and Ge at  $925^\circ\text{C}$ . The 2,2,2-crypt (Merck) was used as received from E. M. Laboratories and handled only in the drybox, as were all the alloys and products. Ethylenediamine (Fisher Scientific Co.) was first dried with  $\text{CaH}_2$ , then distilled onto and stored over molecular sieve, and again distilled from this for utilization. The reaction vessel was equipped with Teflon needle valves (Fischer-Porter). The KGe and  $\text{KGe}_{1.8}$  are slowly reactive with ethylenediamine alone but the process is greatly enhanced by addition of crypt, a brown-yellow solution forming immediately which darkens to deep red-brown. A slight excess of crypt with respect to potassium was generally used. The best crystals of the subject phase, deep-red rods, deposit irreversibly from the solution on long standing. These are fairly brittle and can be cut as necessary. Their composition was determined by x-ray crystallography.

Crystals were selected under the microscope in the drybox, mounted in 0.3 mm diameter thin-wall Lindemann glass capillaries using silicone grease to hold their positions, and checked with brief oscillation photographs. A chunk of dimensions  $0.12 \times 0.28 \times 1.2 \text{ mm}$  which gave the best diffraction spots was investigated on a four-circle automatic diffractometer.

**Data Collection and Reduction.** The preliminary orientation search<sup>17</sup> showed that the crystal was triclinic with a large unit cell, ca.  $8300 \text{ \AA}^3$ . Integrated diffraction intensities were collected at ambient temperature ( $25^\circ\text{C}$ ) via an  $\Omega$  step-scan ( $0.01^\circ$  step, 0.5-s count,  $1^\circ$  scan) in the four octants  $HKL$ ,  $\bar{H}K\bar{L}$ ,  $H\bar{K}L$ ,  $\bar{H}\bar{K}L$  using molybdenum radiation monochromatized with a graphite crystal ( $\lambda$  0.70954  $\text{ \AA}$ ). The reflection data were recorded in two stages, first for 7173 reflections in the range  $0^\circ < 2\theta < 30^\circ$  and later, when the structure appeared solvable, for 9125 reflections with  $30^\circ < 2\theta < 50^\circ$ , each group covering all four octants. During data collection the intensities of three standard reflections were checked after every 75 reflections, and these

**Table I.** Final Positional and Temperature Factor Parameters for Atoms in (2,2,2-crypt K<sup>+</sup>)<sub>6</sub>Ge<sub>9</sub><sup>2-</sup>-Ge<sub>9</sub><sup>4-</sup>-2.5en

	<i>x</i>	<i>y</i>	<i>z</i>	$\beta_{11}^a$	$\beta_{22}$	$\beta_{33}$	$\beta_{12}$	$\beta_{13}$	$\beta_{23}$
Ge11	0.7707 (2)	0.0642 (1)	0.4146 (2)	3.8 (1)	3.0 (1)	7.8 (2)	-0.3 (1)	0.0 (1)	1.6 (1)
Ge12	0.7941 (2)	0.1690 (1)	0.5109 (2)	3.8 (1)	4.2 (1)	6.0 (2)	-1.5 (1)	-0.4 (1)	1.1 (1)
Ge13	0.8530 (2)	0.1220 (1)	0.3755 (2)	2.7 (1)	3.4 (1)	9.4 (3)	-1.1 (1)	0.2 (1)	0.5 (1)
Ge14	0.7019 (2)	0.1148 (1)	0.5375 (2)	5.1 (1)	3.0 (1)	6.2 (2)	-1.2 (1)	0.6 (1)	1.3 (1)
Ge15	0.6696 (2)	0.1861 (1)	0.4557 (3)	4.3 (1)	2.5 (1)	9.8 (3)	0.2 (1)	0.6 (2)	0.8 (1)
Ge16	0.7765 (2)	0.1905 (1)	0.3430 (3)	5.0 (1)	2.9 (1)	9.9 (3)	-1.8 (1)	-0.9 (2)	2.5 (1)
Ge17	0.6487 (2)	0.0934 (1)	0.3680 (2)	2.6 (1)	3.0 (1)	8.2 (2)	-1.2 (1)	0.2 (1)	0.6 (1)
Ge18	0.7533 (2)	0.0959 (1)	0.2573 (2)	3.3 (1)	3.4 (1)	5.4 (2)	-1.0 (1)	0.2 (1)	0.7 (1)
Ge19	0.6622 (2)	0.1608 (1)	0.2781 (3)	5.4 (2)	3.4 (1)	9.7 (3)	-0.7 (1)	-2.1 (2)	2.1 (1)
Ge21	0.1334 (2)	0.3666 (1)	0.0364 (3)	5.3 (2)	3.0 (1)	13.6 (3)	-1.2 (1)	4.5 (2)	0.4 (1)
Ge22	0.2787 (2)	0.3690 (1)	0.1948 (2)	7.2 (2)	2.7 (1)	6.4 (2)	-0.8 (1)	0.1 (2)	1.0 (1)
Ge23	0.2137 (2)	0.3039 (2)	0.0906 (3)	5.8 (2)	4.3 (1)	10.2 (3)	-2.9 (1)	-1.8 (2)	2.9 (1)
Ge24	0.2041 (2)	0.4312 (1)	0.1327 (2)	4.7 (1)	3.7 (1)	6.9 (2)	-0.5 (1)	0.8 (2)	1.1 (1)
Ge25	0.3246 (2)	0.4185 (1)	0.0755 (2)	3.8 (1)	2.4 (1)	9.9 (3)	-1.5 (1)	-0.3 (1)	1.2 (1)
Ge26	0.3321 (2)	0.3240 (1)	0.0526 (3)	4.7 (2)	2.7 (1)	13.9 (4)	-0.1 (1)	2.4 (2)	1.5 (1)
Ge27	0.2102 (2)	0.4170 (1)	0.9531 (2)	4.3 (1)	3.0 (1)	6.9 (2)	-0.9 (1)	-0.3 (1)	2.1 (1)
Ge28	0.2119 (2)	0.3202 (1)	0.9212 (2)	5.1 (1)	3.4 (1)	6.2 (2)	-1.6 (1)	1.0 (2)	-0.4 (1)
Ge29	0.3163 (2)	0.3670 (2)	0.9132 (3)	4.4 (1)	4.3 (1)	8.6 (3)	-1.1 (1)	1.8 (2)	0.4 (1)
K1	0.4532 (3)	0.1070 (2)	0.9228 (4)	2.7 (2)	2.4 (1)	6.4 (4)	-0.7 (1)	-0.3 (2)	1.0 (2)
K2	0.9858 (3)	0.1061 (2)	0.8752 (4)	2.5 (2)	2.6 (1)	6.2 (4)	-0.5 (1)	-0.6 (2)	0.7 (2)
K3	0.3139 (3)	0.1665 (2)	0.4842 (4)	3.3 (2)	2.4 (1)	7.0 (4)	-0.8 (1)	0.2 (3)	1.1 (2)
K4	0.6997 (3)	0.3269 (2)	0.9425 (4)	3.3 (2)	2.0 (1)	5.0 (4)	-0.6 (1)	0.3 (2)	1.2 (2)
K5	0.9870 (3)	0.3798 (2)	0.5032 (4)	2.8 (2)	2.2 (1)	5.6 (4)	-0.9 (1)	0.4 (2)	0.8 (2)
K6	0.6435 (3)	0.4418 (2)	0.3897 (4)	2.7 (2)	2.3 (1)	8.1 (5)	-0.7 (1)	0.1 (3)	0.5 (2)

	<i>x</i>	<i>y</i>	<i>z</i>	<i>B</i>		<i>x</i>	<i>y</i>	<i>z</i>	<i>B</i>
N(101) <sup>b</sup>	0.590 (1)	0.133 (1)	0.882 (2)	7.2 (6)	C(111)	0.280 (2)	0.124 (2)	0.990 (3)	14 (1)
C(102)	0.614 (2)	0.090 (2)	0.801 (4)	15 (2)	C(112)	0.284 (2)	0.164 (1)	0.953 (3)	12 (1)
C(103)	0.571 (2)	0.081 (1)	0.726 (3)	10 (1)	O(113)	0.347 (1)	0.175 (1)	0.926 (2)	12.8 (8)
O(104)	0.510 (1)	0.068 (1)	0.750 (1)	11.5 (7)	C(114)	0.366 (2)	0.215 (2)	0.881 (3)	13 (1)
C(105)	0.469 (2)	0.040 (1)	0.682 (3)	10 (1)	C(115)	0.430 (3)	0.232 (2)	0.892 (4)	16 (2)
C(106)	0.406 (2)	0.037 (1)	0.701 (3)	12 (1)	O(116)	0.476 (1)	0.197 (1)	0.881 (2)	12.0 (7)
O(107)	0.382 (2)	0.047 (1)	0.787 (2)	13.6 (8)	C(117)	0.544 (2)	0.211 (1)	0.898 (3)	10 (1)
C(108)	0.318 (2)	0.029 (1)	0.811 (2)	12 (1)	C(118)	0.591 (2)	0.175 (2)	0.861 (3)	14 (1)
C(109)	0.274 (3)	0.074 (2)	0.869 (4)	16 (2)	C(119)	0.634 (2)	0.123 (1)	0.958 (3)	11 (1)
N(110)	0.316 (2)	0.077 (1)	0.957 (2)	10.8 (8)	C(120)	0.627 (2)	0.089 (2)	0.014 (3)	14 (1)
O(121)	0.561 (1)	0.084 (1)	0.039 (2)	9.8 (6)	C(217)	0.902 (2)	0.133 (1)	0.103 (2)	9.1 (9)
C(122)	0.546 (3)	0.063 (2)	0.116 (4)	14 (1)	C(218)	0.974 (2)	0.118 (1)	0.137 (2)	8.0 (8)
C(123)	0.488 (3)	0.057 (2)	0.140 (3)	13 (1)	C(219)	0.033 (2)	0.186 (1)	0.096 (2)	9.4 (9)
O(124)	0.430 (1)	0.061 (1)	0.075 (2)	10.4 (6)	C(220)	0.072 (2)	0.205 (1)	0.030 (2)	9.1 (9)
C(125)	0.364 (3)	0.053 (2)	0.101 (3)	14 (1)	O(221)	0.033 (1)	0.198 (1)	0.940 (1)	7.6 (5)
C(126)	0.311 (2)	0.056 (1)	0.039 (3)	13 (1)	C(222)	0.065 (2)	0.218 (1)	0.871 (2)	9.2 (9)
N(201)	0.023 (1)	0.135 (1)	0.078 (2)	7.6 (6)	C(223)	0.021 (2)	0.212 (1)	0.785 (3)	10 (1)
C(202)	0.091 (2)	0.107 (1)	0.097 (2)	8.6 (8)	O(224)	0.014 (1)	0.162 (1)	0.745 (2)	10.1 (6)
C(203)	0.093 (2)	0.061 (1)	0.062 (2)	9.1 (9)	C(225)	0.969 (2)	0.159 (1)	0.657 (3)	11 (1)
O(204)	0.094 (1)	0.057 (1)	0.959 (1)	7.9 (5)	C(226)	0.977 (2)	0.108 (1)	0.623 (3)	11 (1)
C(205)	0.103 (2)	0.012 (1)	0.918 (2)	8.1 (8)	N(301)	0.357 (2)	0.264 (1)	0.549 (2)	9.8 (7)
C(206)	0.108 (2)	0.004 (1)	0.812 (2)	8.3 (8)	C(302)	0.430 (2)	0.264 (1)	0.544 (2)	10 (1)
O(207)	0.041 (1)	0.021 (1)	0.779 (2)	9.5 (6)	C(303)	0.470 (2)	0.227 (1)	0.572 (2)	8.7 (9)
C(208)	0.041 (2)	0.014 (1)	0.674 (2)	12 (1)	O(304)	0.449 (1)	0.187 (1)	0.522 (2)	9.2 (6)
C(209)	0.965 (2)	0.028 (1)	0.650 (3)	11 (1)	C(305)	0.492 (2)	0.150 (1)	0.537 (3)	11 (1)
N(210)	0.947 (2)	0.077 (1)	0.672 (2)	9.9 (7)	C(306)	0.478 (2)	0.108 (1)	0.471 (2)	8.9 (9)
C(211)	0.872 (2)	0.084 (1)	0.661 (3)	11 (1)	O(307)	0.409 (1)	0.092 (1)	0.479 (1)	9.1 (6)
C(212)	0.835 (2)	0.057 (1)	0.726 (3)	11 (1)	C(308)	0.397 (2)	0.048 (1)	0.430 (3)	11 (1)
O(213)	0.849 (1)	0.087 (1)	0.822 (1)	7.0 (4)	C(309)	0.327 (2)	0.034 (1)	0.444 (2)	9.6 (9)
C(214)	0.819 (2)	0.066 (1)	0.895 (2)	8.1 (8)	N(310)	0.275 (1)	0.066 (1)	0.418 (2)	8.1 (6)
C(215)	0.821 (2)	0.100 (1)	0.978 (2)	7.8 (8)	C(311)	0.212 (2)	0.058 (1)	0.458 (3)	11 (1)
O(216)	0.894 (1)	0.100 (1)	0.013 (1)	7.9 (5)	C(312)	0.216 (2)	0.076 (1)	0.569 (2)	8.7 (9)
O(313)	0.217 (1)	0.125 (1)	0.579 (1)	7.7 (5)	N(410)	0.830 (1)	0.273 (1)	0.967 (2)	7.4 (6)
C(314)	0.218 (2)	0.147 (1)	0.674 (2)	7.7 (8)	C(411)	0.825 (2)	0.228 (1)	0.908 (2)	7.8 (8)
C(315)	0.210 (2)	0.198 (1)	0.684 (2)	10 (1)	C(412)	0.799 (2)	0.232 (1)	0.804 (2)	9.5 (9)
O(316)	0.272 (1)	0.213 (1)	0.652 (1)	8.8 (5)	O(413)	0.736 (1)	0.251 (1)	0.811 (1)	8.1 (5)
C(317)	0.271 (2)	0.263 (1)	0.670 (3)	10 (1)	C(414)	0.708 (2)	0.254 (1)	0.712 (2)	8.8 (9)
C(318)	0.337 (2)	0.278 (1)	0.644 (3)	12 (1)	C(415)	0.639 (2)	0.267 (1)	0.714 (2)	9.1 (9)
C(319)	0.314 (2)	0.296 (1)	0.495 (3)	11 (1)	O(416)	0.626 (1)	0.311 (1)	0.766 (1)	7.1 (5)
C(320)	0.315 (2)	0.278 (1)	0.390 (3)	11 (1)	C(417)	0.559 (1)	0.328 (1)	0.766 (2)	6.7 (7)
O(321)	0.278 (1)	0.235 (1)	0.373 (2)	11.3 (7)	C(418)	0.549 (1)	0.374 (1)	0.817 (2)	7.5 (8)
C(322)	0.275 (2)	0.219 (2)	0.267 (3)	14 (1)	C(419)	0.584 (2)	0.431 (1)	0.968 (2)	8.1 (8)
C(323)	0.234 (2)	0.175 (2)	0.251 (3)	13 (1)	C(420)	0.642 (2)	0.451 (1)	0.931 (2)	11 (1)
O(324)	0.263 (1)	0.140 (1)	0.292 (2)	10.5 (6)	O(421)	0.699 (1)	0.423 (1)	0.954 (3)	7.4 (5)
C(325)	0.230 (2)	0.096 (2)	0.287 (3)	12 (1)	C(422)	0.760 (2)	0.439 (1)	0.919 (2)	10 (1)
C(326)	0.269 (2)	0.059 (1)	0.311 (3)	11 (1)	C(423)	0.819 (1)	0.423 (1)	0.974 (2)	6.0 (7)

Table I (Continued)

	<i>x</i>	<i>y</i>	<i>z</i>	<i>B</i>		<i>x</i>	<i>y</i>	<i>z</i>	<i>B</i>
N(401)	0.571 (1)	0.380 (1)	0.921 (1)	6.2 (5)	O(424)	0.823 (1)	0.372 (1)	0.945 (1)	6.8 (5)
C(402)	0.517 (1)	0.361 (1)	0.971 (1)	6.6 (7)	C(425)	0.879 (1)	0.352 (1)	0.986 (2)	6.8 (7)
C(403)	0.544 (2)	0.352 (1)	0.065 (2)	7.7 (8)	C(426)	0.889 (2)	0.303 (1)	0.954 (2)	9.3 (9)
O(404)	0.595 (1)	0.318 (1)	0.058 (1)	5.6 (4)	N(501)	0.927 (1)	0.390 (1)	0.692 (2)	8.1 (6)
C(405)	0.618 (1)	0.312 (1)	0.150 (2)	6.1 (7)	C(502)	0.980 (2)	0.373 (1)	0.756 (2)	9.0 (9)
C(406)	0.664 (1)	0.270 (1)	0.141 (2)	6.1 (7)	C(503)	0.043 (2)	0.397 (1)	0.759 (2)	9.5 (9)
O(407)	0.726 (1)	0.284 (1)	0.101 (1)	6.4 (4)	O(504)	0.072 (1)	0.376 (1)	0.668 (1)	9.0 (6)
C(408)	0.777 (2)	0.247 (1)	0.106 (2)	8.1 (8)	C(505)	0.144 (2)	0.389 (1)	0.654 (3)	11 (1)
C(409)	0.838 (2)	0.266 (1)	0.066 (2)	9.2 (9)	C(506)	0.164 (2)	0.362 (1)	0.565 (2)	8.4 (8)
O(507)	0.128 (1)	0.387 (1)	0.499 (2)	9.0 (6)	O(604)	0.729 (1)	0.366 (1)	0.334 (2)	9.8 (6)
C(508)	0.150 (2)	0.371 (1)	0.405 (3)	10.6 (1)	C(605)	0.791 (2)	0.373 (1)	0.292 (2)	9.3 (9)
C(509)	0.112 (2)	0.392 (1)	0.336 (2)	8.9 (9)	C(606)	0.774 (2)	0.407 (1)	0.234 (3)	11 (1)
N(510)	0.040 (1)	0.372 (1)	0.318 (2)	7.0 (6)	O(607)	0.752 (1)	0.450 (1)	0.278 (2)	10.8 (6)
C(511)	0.046 (2)	0.324 (1)	0.271 (2)	9.3 (9)	C(608)	0.747 (2)	0.487 (2)	0.224 (3)	13.8 (1)
C(512)	0.981 (2)	0.296 (1)	0.277 (2)	8.7 (9)	C(609)	0.714 (2)	0.525 (2)	0.265 (3)	12 (1)
O(513)	0.978 (1)	0.294 (1)	0.374 (1)	7.0 (5)	N(610)	0.650 (2)	0.526 (1)	0.298 (3)	14 (1)
C(514)	0.925 (2)	0.264 (1)	0.391 (2)	8.1 (8)	C(611)	0.602 (3)	0.514 (2)	0.203 (4)	15 (2)
C(515)	0.920 (2)	0.266 (1)	0.487 (2)	8.3 (8)	C(612)	0.535 (3)	0.504 (2)	0.242 (3)	15 (1)
O(516)	0.902 (1)	0.310 (1)	0.535 (1)	8.5 (5)	O(613)	0.537 (2)	0.458 (1)	0.262 (2)	13.7 (8)
C(517)	0.890 (2)	0.306 (1)	0.629 (3)	11 (1)	C(614)	0.476 (3)	0.439 (2)	0.295 (3)	15 (1)
C(518)	0.874 (2)	0.355 (1)	0.674 (2)	9.4 (9)	C(615)	0.482 (2)	0.398 (2)	0.305 (3)	12 (1)
C(519)	0.906 (2)	0.439 (1)	0.720 (2)	8.6 (9)	O(616)	0.520 (1)	0.395 (1)	0.394 (2)	12.1 (7)
C(520)	0.863 (2)	0.461 (1)	0.649 (3)	10 (1)	C(617)	0.530 (2)	0.349 (1)	0.410 (3)	10 (1)
O(521)	0.906 (1)	0.460 (1)	0.566 (1)	8.2 (5)	C(618)	0.570 (3)	0.353 (2)	0.499 (4)	15 (1)
C(522)	0.868 (2)	0.480 (1)	0.499 (2)	9 (1)	C(619)	0.692 (2)	0.368 (2)	0.583 (3)	13 (1)
C(523)	0.915 (2)	0.486 (1)	0.418 (2)	8.4 (8)	C(620)	0.666 (2)	0.410 (1)	0.628 (3)	11 (1)
O(524)	0.940 (1)	0.442 (1)	0.384 (1)	7.8 (5)	O(621)	0.689 (1)	0.449 (1)	0.586 (2)	11.5 (7)
C(525)	0.982 (2)	0.449 (1)	0.306 (2)	8.4 (9)	C(622)	0.676 (3)	0.491 (2)	0.634 (4)	18 (2)
C(526)	0.027 (2)	0.402 (1)	0.257 (2)	9.1 (9)	C(623)	0.689 (2)	0.529 (1)	0.599 (3)	12 (1)
N(601)	0.643 (2)	0.353 (1)	0.477 (2)	12.1 (9)	O(624)	0.654 (1)	0.531 (1)	0.509 (2)	13.9 (8)
C(602)	0.677 (2)	0.318 (2)	0.416 (3)	13 (1)	C(625)	0.663 (3)	0.563 (2)	0.509 (2)	13.9 (8)
C(603)	0.743 (2)	0.329 (2)	0.382 (3)	13 (1)	C(626)	0.625 (3)	0.568 (2)	0.368 (5)	20 (2)
N11 <sup>c</sup>	0.104 (2)	0.236 (2)	0.464 (3)	19 (1)					
C11	0.109 (4)	0.185 (3)	0.434 (6)	26 (3)					
C12	0.052 (3)	0.166 (2)	0.415 (4)	19 (2)					
N12	0.053 (2)	0.115 (2)	0.394 (3)	19 (1)					
N21	0.511 (4)	0.236 (3)	0.313 (5)	32 (3)					
C21	0.467 (3)	0.188 (2)	0.279 (4)	20 (2)					
C22	0.471 (4)	0.228 (3)	0.180 (6)	25 (3)					
N22	0.454 (5)	0.187 (3)	0.135 (7)	37 (4)					
N31	0.974 (4)	0.504 (4)	0.059 (6)	35 (3)					
C31	0.0150 (5)	0.469 (3)	0.031 (7)	25 (3)					

<sup>a</sup>  $\beta_{ij} \times 10^3$  is listed. The thermal parameter expression is  $\exp[-(h^2\beta_{11} + k^2\beta_{22} + l^2\beta_{33} + 2hk\beta_{12} + 2hl\beta_{13} + 2kl\beta_{23})]$ . <sup>b</sup> The first digit keys on the crypt cation, the second and third on the atoms therein in the order given in Figure 3 and ref 12. <sup>c</sup> Atoms in ethylenediamine molecules.

were retained if any substantial loss in intensity was observed. The necessity of changing the three standard reflections during data collection because of a significant decrease in intensity owing to crystal decomposition yielded four separate data sets. Each was corrected for isotropic decay through a least-squares fitting of a third-order polynomial to the measured standard intensity sum as a function of reflection count. These sets were separately corrected for Lorentz and polarization effects and, once the composition of the compound was known, for absorption, ( $\mu = 36 \text{ cm}^{-1}$ ), the transmission coefficients ranging from 0.36 to 0.63. The four data sets were then merged and duplicate reflections averaged, with each set being assigned a separate flag so that these could be scaled one to another with four refined scale factors.

From a total of 16 298 recorded reflections, 8461 with  $I > 3\sigma(I)$  and  $F > 3\sigma(F)$  were kept as observed, the errors being defined as before.<sup>12</sup> The initial structure solution and preliminary refinements were carried out with the 5980 reflections in the first two data sets ( $2\theta < 30^\circ$ ) while all data were employed for final refinement cycles. A Howells-Phillips-Rogers test gave a strong indication of centrality. Precise lattice dimensions were obtained by least-squares fitting of the  $2\theta$  values obtained from the data crystal by tuning on both Friedel-related peaks for eight known reflections which had  $20^\circ < 2\theta < 30^\circ$ , giving constants of  $a = 20.037 (2) \text{ \AA}$ ,  $b = 28.994 (2) \text{ \AA}$ ,  $c =$

$14.546 (2) \text{ \AA}$ ,  $\alpha = 99.356 (8)^\circ$ ,  $\beta = 94.077 (8)^\circ$ ,  $\gamma = 87.60 (1)^\circ$ ,  $V = 8312.9 (12) \text{ \AA}^3$ .

Programs and procedures and the source of scattering factor data were as previously referenced.<sup>12,18</sup> The neutral atom scattering factors used included corrections for the real and imaginary parts of anomalous dispersion.

**Structure Solution and Refinement.** The heavy atoms were readily located by direct methods. The output from the Fourier step of MULTAN<sup>18</sup> contained 18 large peaks which described two clusters in the asymmetric unit, each having interpeak distances on the order of 2.6  $\text{\AA}$ . After a few cycles of positional and isotropic thermal parameter refinement  $R = \Sigma||F_o| - |F_c||/\Sigma|F_o| = 0.43$ . At this stage, an electron density map contained, in addition to the 18 germanium atoms, six new peaks of appropriate height and location to be attributed to potassium atoms plus a few smaller peaks around them indicative of carbon, oxygen, and nitrogen atoms of the crypt ligand. After a few successive refinements of these positions by block diagonal least squares followed by electron density synthesis the positions of all of the atoms in the six crypt-K<sup>+</sup> cations had been defined. Final refinement of the complete structure was conducted in parts using all 8461 data and full matrix least squares techniques with a locally expanded version of ORFLS. To reduce the computing time and cost, the 190 atoms were refined to convergence by cycling several times

**Table II.** Bond Distances, Angles, and Dihedral Angles in Cluster I, Ge<sub>9</sub><sup>2-</sup>

Germanium atoms	<i>d</i> , Å	Germanium atoms	<i>d</i> , Å
1-2	3.170 (5)	5-7	2.811 (6)
1-3	2.554 (5)	5-9	2.565 (6)
1-4	2.565 (5)	6-8	2.857 (6)
1-7	2.634 (5)	6-9	2.528 (6)
1-8	2.599 (4)	7-8	2.742 (5)
2-3	2.540 (6)	7-9	2.553 (5)
2-4	2.565 (6)	8-9	2.571 (7)
2-5	2.621 (6)	3-9	4.158 (8)
2-6	2.616 (5)	4-9	4.217 (6)
3-6	2.551 (7)	3-4	4.001 (6)
3-8	2.596 (5)	5-8	3.980 (8)
4-5	2.584 (6)	6-7	3.944 (7)
4-7	2.604 (5)	1-9	4.149 (7)
5-6	2.795 (6)	2-9	4.129 (6)

Atoms	Angle, deg	Atoms	Angle, deg
3-1-8	60.5 (1)	5-2-6	64.5 (2)
3-1-2	51.3 (1)	5-2-4	59.8 (2)
2-1-8	87.0 (1)	1-2-4	51.8 (1)
2-1-4	51.8 (1)	3-2-4	103.2 (2)
4-1-7	60.1 (1)	1-3-8	60.6 (1)
7-1-8	63.2 (1)	1-3-2	77.0 (1)
3-1-4	102.8 (1)	2-3-6	61.8 (2)
3-2-1	51.8 (1)	6-3-8	67.4 (2)
3-2-6	59.3 (2)	1-4-2	76.3 (2)
1-2-6	86.1 (2)	2-4-5	61.2 (2)
5-4-7	65.6 (2)	8-7-9	57.7 (2)
1-4-7	61.3 (1)	1-7-5	93.8 (2)
4-5-7	57.5 (1)	1-7-8	57.8 (1)
2-5-4	59.0 (2)	1-7-4	58.6 (2)
2-5-7	94.0 (2)	4-7-5	56.9 (2)
2-5-6	57.7 (1)	3-8-6	55.5 (2)
6-5-9	56.1 (2)	3-8-1	58.9 (1)
7-5-9	56.5 (2)	1-8-6	93.3 (2)
6-5-7	89.4 (2)	1-8-7	59.0 (1)
3-6-8	57.0 (2)	7-8-6	89.5 (2)
3-6-2	58.9 (2)	7-8-9	57.4 (2)
2-6-8	93.6 (2)	6-8-9	55.3 (2)
2-6-5	57.9 (1)	5-9-6	66.6 (2)
5-6-9	57.4 (2)	6-9-8	68.3 (2)
8-6-9	56.4 (2)	7-9-8	64.8 (2)
5-6-8	89.5 (2)	5-9-7	66.6 (2)
5-7-8	91.5 (2)	6-9-7	101.8 (2)
5-7-9	56.9 (1)	5-9-8	101.8 (2)

Atoms	Angle, deg	Atoms	Angle, deg
(7-8-1) (5-2-6)	171.2 (1)	(4-7-1) (7-8-1)	43.6 (1)
(4-1-2) (9-6-8)	133.6 (2)	(7-8-1) (1-8-3)	46.6 (2)
(7-1-4) (9-5-6)	139.6 (1)	(1-8-3) (3-8-6)	60.3 (2)
(7-9-8) (4-2-5)	139.1 (2)	(3-8-6) (6-2-3)	61.4 (2)
(7-4-5) (7-5-9)	24.9 (2)	(6-2-3) (2-6-5)	45.3 (2)
(3-8-6) (7-4-5)	146.9 (2)	(2-6-5) (2-5-4)	45.2 (2)
(1-8-3) (5-4-2)	141.9 (2)	(2-5-4) (4-5-7)	61.5 (2)
(2-1-3) (2-4-1)	8.3 (2)	(4-5-7) (4-7-1)	60.6 (2)
(9-7-5) (2-1-3)	136.0 (2)	(7-9-8) (7-8-1)	38.0 (2)
(9-6-8) (6-3-8)	23.3 (2)	(6-9-5) (6-5-2)	36.1 (2)

first for 18 germanium atoms and then among pairs of the six crypt-K<sup>+</sup> cations. Germanium and potassium were ultimately refined with anisotropic thermal parameters while light atoms in the ligands were restricted to isotropic thermal parameters. Toward the end of the refinement an electron density difference map indicated the presence of 2.5 solvent molecules in the asymmetric unit cell, the 0.5 fraction originating from the presence of one en in the hole at the center of symmetry. The peaks from solvent molecules were in general broad suggesting a weak bonding and a significant disorder (or thermal motion) of the molecules. A total of 236 hydrogen atoms in the asymmetric unit, representing 12% of the total electron density, were not located or their estimated positions included in the structure factor calculations.

**Table III.** Bond Distances, Angles, and Dihedral Angles in Cluster 2, Ge<sub>9</sub><sup>4-</sup>

Germanium atoms	<i>d</i> , Å	Germanium atoms	<i>d</i> , Å
1-3	2.561 (7)	5-9	2.578 (6)
1-4	2.562 (7)	6-8	2.962 (7)
1-7	2.646 (6)	6-9	2.544 (6)
1-8	2.561 (6)	7-8	2.764 (6)
2-3	2.557 (6)	7-9	2.569 (7)
2-4	2.533 (7)	8-9	2.560 (6)
2-5	2.659 (5)	1-2	3.580 (7)
2-6	2.538 (7)	3-4	3.638 (7)
3-6	2.585 (6)	6-7	3.943 (8)
3-8	2.583 (5)	5-8	3.997 (8)
4-5	2.601 (6)	9-3	4.105 (7)
4-7	2.590 (5)	4-9	4.178 (8)
5-6	2.703 (6)	1-9	4.197 (7)
5-7	2.799 (6)	2-9	4.211 (6)

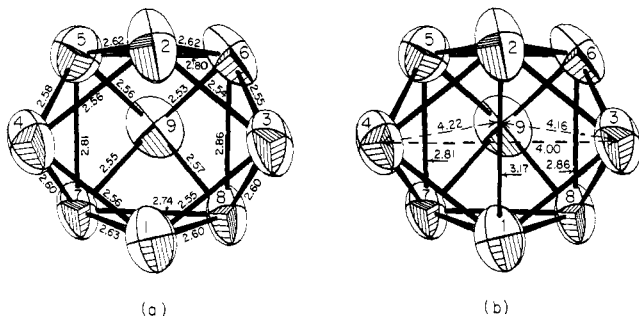
Atoms	Angle, deg	Atoms	Angle, deg
8-1-3	60.6 (2)	6-3-2	59.2 (2)
8-1-7	64.1 (2)	6-3-8	69.9 (2)
4-1-7	59.6 (2)	8-3-1	59.7 (2)
4-1-3	90.5 (2)	1-3-2	88.8 (2)
4-2-3	91.2 (2)	1-4-7	61.8 (2)
6-2-3	61.0 (2)	5-4-7	65.3 (2)
6-2-5	62.7 (2)	5-4-2	62.4 (2)
5-2-4	60.1 (2)	1-4-2	89.3 (2)
4-5-2	57.6 (2)	5-7-9	57.2 (2)
2-5-6	56.5 (2)	5-7-4	57.6 (1)
6-5-9	57.5 (2)	8-7-5	91.8 (2)
6-5-7	91.6 (2)	6-8-7	87.0 (2)
7-5-9	56.9 (2)	6-8-9	54.3 (2)
4-5-7	57.2 (1)	7-8-9	57.6 (2)
4-5-6	98.6 (2)	1-8-7	59.4 (2)
8-6-9	54.8 (2)	1-8-3	59.7 (2)
8-6-3	55.0 (1)	6-8-3	55.1 (1)
5-6-9	58.8 (2)	8-9-7	65.2 (2)
5-6-2	60.9 (2)	8-9-6	70.9 (2)
2-6-3	59.9 (2)	6-9-5	63.7 (2)
5-6-8	89.6 (2)	5-9-7	65.9 (2)
8-7-1	56.4 (2)	8-9-5	102.1 (2)
8-7-9	57.2 (2)	6-9-7	100.9 (2)
1-7-4	58.6 (2)		

Atoms	Angle, deg	Atoms	Angle, deg
(8-6-3) (4-5-7)	155.6 (2)	(4-7-1) (7-8-1)	51.0 (2)
(3-6-2) (4-7-1)	143.9 (2)	(7-8-1) (1-8-3)	54.4 (2)
(3-1-8) (2-5-4)	143.0 (2)	(1-8-3) (8-6-3)	55.7 (2)
(2-6-5) (8-1-7)	161.6 (2)	(8-6-3) (3-6-2)	53.6 (2)
(1-3-2) (2-4-1)	5.3 (2)	(3-6-2) (6-5-2)	53.0 (2)
(1-7-8) (7-9-8)	32.1 (2)	(6-5-2) (5-4-2)	50.8 (2)
(9-5-6) (5-2-6)	33.2 (2)	(5-4-2) (5-7-4)	52.9 (2)
(5-9-7) (5-7-4)	32.0 (2)	(5-7-4) (4-7-1)	52.7 (2)
(9-6-8) (6-3-8)	23.9 (2)		

Convergence was obtained with  $R = 0.149$ ,  $R_w = 0.169 = (\sum w\Delta^2 / \sum wF_o^2)^{1/2}$ ,  $w = \sigma_F^{-2}$ , for 884 variables and 8409 reflections within the range  $0^\circ < 2\theta < 50^\circ$ , 52 of the weakest and evidently mismeasured reflections being eliminated at that point by the criterion  $||F_c| - F_o|/F_o > 1.1$ . The final electron density difference map was flat except for a very few areas with a background of  $\pm 1 e/\text{\AA}^3$ . In the final cycle refinement the shift in heavy atom parameters was  $\leq 0.09\sigma$  in positions and  $0.3\sigma$  in temperature factors while the changes in light atom parameters were  $\leq 0.4\sigma$ .

At first glance, such simple criteria of "goodness" as the magnitude of the residuals suggest that the structure may not be particularly well defined, but according to more pertinent quantities the results appear very acceptable indeed. Thus the final positional uncertainties found for all atoms in this structure are in comparison as good as or better than those obtained in other recent and relatively large structural problems involving alkali metal-crypt derivatives of  $\text{Sb}_7^{3-}$ ,  $\text{Sn}_9^{4-}$ , and  $\text{Te}_3^{2-}$  where all atoms are in general positions.<sup>10,12,13</sup> The esd's



**Figure 1.** Two views of cluster 1,  $\text{Ge}_9^{2-}$ , in the compound  $(2,2,2\text{-crypt-K}^+)_6\text{Ge}_9^{2-}\text{-Ge}_9^{4-}\cdot 2.5\text{en}$ .

for the individual Ge positions, 0.0030–0.0046 Å, compare favorably with those obtained with the *heavier* Sn, Sb, and Te, 0.0026–0.0051 Å, while the uncertainties in the positions of N and O (0.016–0.042 Å), C (0.02–0.06 Å), and K (0.006–0.007 Å) are also less than those for the cryptated cations in these other structures even when esd's for the evidently disordered ligand carbon atoms encountered earlier are discounted. Thus the literally less satisfying value of residuals must arise primarily from the occurrence of larger random errors in the data set, presumably originating mostly from the 80% intensity decay encountered during data collection. For example, any anisotropy in the decay of intensities would not be corrected by the procedures used, while many normally observable reflections were presumably missed in the last part of the data collection ( $30^\circ < 2\theta < 50^\circ$ ). The residuals drop to 0.130 and 0.131 when data with  $2\theta > 33^\circ$  are excluded from the calculation. In view of the foregoing considerations an improvement in the precision and thence in the possible value of the results through collection of data from a cooled crystal, or from several crystals, were judged to clearly not be worth the sizable cost involved.

## Results and Discussion

The final positional and thermal parameters for the 190 nonhydrogen atoms in  $(\text{crypt-K}^+)_6\text{Ge}_9^{2-}\text{-Ge}_9^{4-}\cdot 2.5\text{en}$  are listed in Table I. Bond distances, bond angles, and dihedral angles in the nine atom clusters 1 and 2 are given in Tables II and III, respectively. Bond distance and angle data for the crypt-potassium cations (Table A), a listing of the shorter interionic distances in the structure (Table B), and a tabulation of calculated and observed structure factor amplitudes are included in the supplementary material. The configurations of the  $\text{Ge}_9$  anions 1 and 2 are illustrated in Figures 1 and 2, respectively, while Figure 3 illustrates the crypt- $\text{K}^+$  cation (4) from two different views. A stereoscopic [001] view of the packing in the unit cell is given in Figure 4, the arrangement being simplified by excluding the carbon atoms in the cations as well as the five solvent molecules. A layering of the cations is evident.

The structures found here for all the crypt-potassium cations are comparable to those determined for similar symmetry-unconstrained units in  $(\text{crypt-K}^+)_2\text{Te}_3^{2-}$ .<sup>13</sup> Likewise the K–O distances, 2.76 (2) to 2.92 (3) Å, and K–N distances, 2.95 (2) to 3.04 (3) Å, as well as those within the ligand (Table A), again exhibit a wider range than those reported earlier<sup>20</sup> in crypt- $\text{K}^+\text{I}^-$  but there is no evidence of a reduction from 8 to 6 coordination found on rare occasion at least with the smaller sodium ion and 2,2,2-crypt.<sup>2</sup> The closest approach of nitrogen atoms in en to any atom in the cluster, 3.67 Å (Table B), suggests that hydrogen bonding between the two is not important.

Certainly the most remarkable feature of the structure is the presence of two different anionic clusters containing nine germanium atoms each. Because the structure clearly contains six cryptated cations in the independent unit the two anions together must support a negative charge of 6. The first possibility would be to attribute to each cluster a charge of 3–; however, there is no precedent for an odd number of electrons

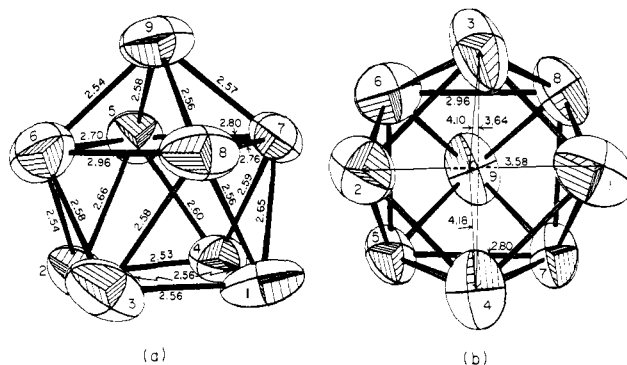


**Figure 2.** Two views of cluster 2,  $\text{Ge}_9^{4-}$ . Thermal ellipsoids are all shown at the 50% probability level.

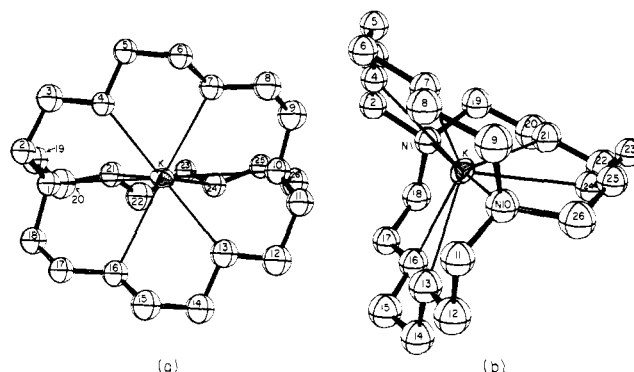


**Figure 3.** The crypt- $\text{K}^+$  (4) cation in  $(\text{crypt-K}^+)_6\text{Ge}_9^{2-}\text{-Ge}_9^{4-}\cdot 2.5\text{en}$ . (a) N–K–N axis horizontal. (b) Tilted for a nearer end-on view from N10.

in a radical ion cluster. A much more probable answer is the presence of one cluster with a charge of 2– and a second with a charge of 4–. Such a difference of charge would be expected to introduce a substantial difference in geometric configuration of the two clusters, and in fact these differences can be perceived and allow a fairly straightforward assignment of a 2– charge to cluster 1 and a 4– charge to cluster 2. This distinction is also supported by MO calculations.

Visual comparison of the clusters from various perspectives is not sufficient to allow a clear differentiation, but a brief consideration of selected distances does provide a reasonable disposition of the charge, and a comparison of dihedral angles gives a more quantitative statement of the same conclusion. The perspectives in the clusters shown in Figures 1 and 2 were selected to emphasize the conclusions, but in any case it should be remembered that the geometric differences between not just these clusters but the pertinent  $D_{3h}$  and  $C_{4v}$  limits for nine atom polyhedra as well are not very large.<sup>2,21,22</sup> In terms of Figure 1a the most direct conversion of cluster 1, which is nearer to  $D_{3h}$ , to the  $C_{4v}$  extreme (via  $C_{2v}$ ) involves a distortion in which the four closest atoms 1, 2, 3, 4 become planar and form a square with the generation of a fourfold axis away from the viewer through Ge-9. This also requires that the shortest distances between atoms 5, 6, 7, 8 which originally defined the height of the  $D_{3h}$  prism and edges of its caps become equal in the upper square of the antiprism. Conversely cluster 2, Figure 2a, will go from close to  $C_{4v}$  toward  $D_{3h}$  most directly by development of a horizontal prismatic threefold axis through parallel caps 2, 5, 6 and 1, 7, 8 while the square base folds and compresses along 1–2 as atoms 3, 4, and 9 become equivalent capping atoms.

Inspection of the nearest-neighbor distances in Figures 1a and 2a provides little assistance in classification, but some second nearest-neighbor distances do, particularly those that define the degree of squareness of the base in  $C_{4v}$  vs. the dis-

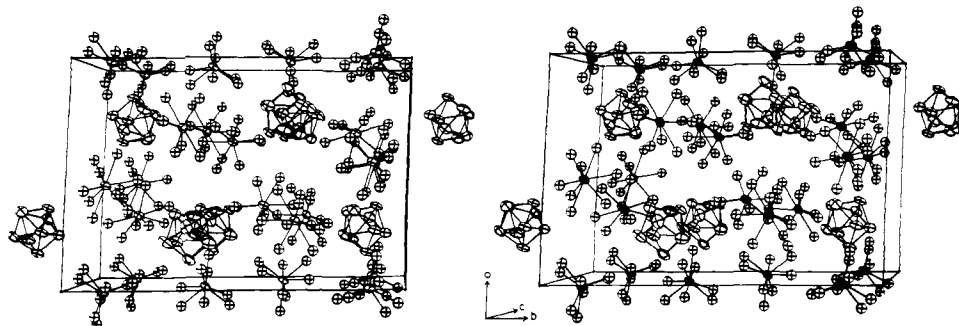


Figure 4. Stereoview of the unit cell of  $(\text{crypt-K}^+)_6\text{Ge}_9^{2-}\text{Ge}_9^{4-}\cdot 2.5\text{en}$ , including ions from a second formula unit related by translation. Solvent molecules, carbon atoms in the cations, and hydrogen atoms are excluded. Cluster 2 occurs nearer the body center.

Table IV. Some Dihedral Angles in Nine Atom Polyhedra<sup>a</sup>

Type face	Example, Figure 1 $\delta$ , $\text{Bi}_9^{5+ b}$	Trigonal prism (opposed)	Cap to cap (vicinal)	Prism end to cap (vicinal)							
		(1-7-8, 2-6-5)	(1-2-4, 1-3-2)	(1-7-8, 1-4-7)							
$D_{3h}$		180°	22° (x3)	43° (x6)							
$C_{2v}$	$\delta$ , $\text{Bi}_9^{5+ c}$	174°	14°	24° (x2)	41°	43°	48° (x4)				
$C_{2v}$	$\delta$ , $\text{Ge}_9^{2+ d}$	171°	8°	25°	23°	38°	36°	44°	47°	45°	45°
$C_{4v}$	$\delta$ , $\text{Ge}_9^{4+ d}$	162°	5°	32°	24°	32°	33°	51°	54°	53°	51°
$C_{4v}$	$\delta$ , $\text{Sn}_9^{4+ e}$	158° (x2)	3°	30°	29° (x2)	32°	32°	52°	53°	54°	55°
Type face		Opposed, waist	Base	Cap to antiprism			Vicinal, waist				

<sup>a</sup>Vicinal angles around capping atoms 3, 4, 9 are not included. <sup>b</sup>Reference 23. <sup>c</sup>Reference 24. <sup>d</sup>This work. <sup>e</sup>Reference 2.

tances between equivalent capping atoms 3-4-9 in  $D_{3h}$  and the equality of the three edges defining the height of the trigonal prism. Pertinent values are shown in Figures 1b and 2b. The clearest assignment comes with cluster 2, where dimensions all seem appropriate to a symmetry rather close to  $C_{4v}$ . By its close analogy to  $\text{Sn}_9^{4-}$ ,<sup>2</sup> cluster 2 is therefore assigned as  $\text{Ge}_9^{4-}$ . The most direct evidence is the near equality of the diagonals of the square base, 3.58 and 3.64 Å for 1-2 and 3-4, respectively, together with the facts that the angles therein are within 1.2° ( $6\sigma$ ) of 90° and the base is close to planar, with an upward fold of only 5.3° about 1-2 (Table III). A substantial distinction from  $D_{3h}$  symmetry is indicated by the disparity between what in  $D_{3h}$  would be equivalent distances, the parallel edges of the trigonal prism, 2.80, 2.96, and 3.58 Å for 6-8, 5-7, and 1-2, respectively, as well as the distances between the capping atoms, the 1-9 and 2-9 separations being more than 0.5 Å longer than the third, 3-4 (Figure 2b). (The alternate selection of prism 4-5-7, 3-6-8 with capping atoms 1-2-9 is somewhat less applicable and it is contrary to the 5° fold about 1-2.)

Although the distortion of cluster 1 from its  $D_{3h}$  parent is relatively greater, the evidence still seems clear that it derives from that limit. Referring to Figure 1b the three edges which would best describe the height of a trigonal prism are moderately similar, 2.81, 2.86, and 3.17 Å, and the three capping atoms (3, 4, 9) are nearly equally separated at 4.22, 4.16, and, across the near face, 4.00 Å. Thus the distortion found clearly seems to be along the  $C_{2v}$  pathway from  $D_{3h}$  toward, but still a moderate way from,  $C_{4v}$ . The face 1-3-2-4 has bond angles near 77 and 103° and appears distorted toward a square by changes in the diagonals of about 0.2 Å, or roughly 1/3 of the way toward the  $C_{4v}$  limit presuming no important changes in

bond length with cluster charge. On the basis of the above considerations cluster 1 is concluded to be  $\text{Ge}_9^{2-}$ .

As has been discussed before,<sup>2,21</sup> dihedral angles provide a better quantification of the degree and character of distortions from ideal models. The major changes in selected dihedral angles involving the two germanium clusters as they relate to  $\text{Sn}_9^{4-}$  at one extreme and  $\text{Bi}_9^{5+}$  at the other are compared in Table IV. Critical quantities in the present case are the dihedral angles  $\delta$  between the opposite faces of the trigonal prism (1-7-8 and 2-5-6) which are 180° for the ideal  $D_{3h}$  reducing to 171° in cluster 1, 162° in cluster 2, and 158° in the  $C_{4v}$  example of  $\text{Sn}_9^{4-}$ . For the alternate prism 4-5-7, 3-6-8 in cluster 2,  $\delta$  is 156° vs. 158° in  $\text{Sn}_9^{4-}$ , and this reduces to 134, 136, and 147° in cluster 1 and 142° in  $\text{Bi}_9^{5+}$  for the three equivalent pairs of opposed faces parallel to the threefold axis.<sup>23</sup> Likewise, the dihedral angles between vicinal triangles between capping atoms (e.g., 1-2-4 and 1-2-3) start at 22° in  $\text{Bi}_9^{5+}$  and diverge, one pair decreasing to 8° in 1, 5° in 2, and 3° in  $\text{Sn}_9^{4-}$  as the base approaches a square.

With respect to electronic configurations the close correspondence between the configurations of the isoelectronic  $\text{Ge}_9^{4-}$  and  $\text{Sn}_9^{4-}$ , each with 22 cage electrons, has already been invoked in the assignments, and a similar relationship is to be found between  $\text{Ge}_9^{2-}$  and  $\text{B}_9\text{H}_9^{2-}$ ,<sup>25</sup> both with  $D_{3h}$  symmetry. However, this seemingly simple classification is at odds with the  $D_{3h}$  symmetry of the 22-electron  $\text{Bi}_9^{5+}$  in the compound  $\text{Bi}^+\text{Bi}_9^{5+}(\text{HfCl}_6^{2-})_3$ <sup>23</sup> plus a  $C_{2v}$  version of the same ion in  $\text{Bi}_{12}\text{Cl}_{14}$ <sup>24,26</sup> which appears to be distorted about 25% of the way from  $D_{3h}$  more or less toward  $C_{4v}$ .<sup>2</sup> Though  $\text{Bi}_9^{5+}$  now lacks one pair of approximately nonbonding ( $a_2''$ ) electrons of  $\text{B}_9\text{H}_9^{2-}$ ,<sup>27</sup> this seemingly has little influence on the symmetry, although it must be admitted that the elements involved

differ by four periods. On the other hand, the contrast between a  $D_{3h}$   $\text{Bi}_9^{5+}$  and the isoelectronic but  $C_{4v}$   $\text{Sn}_9^{4-}$  and  $\text{Ge}_9^{4-}$  is a bit more puzzling, although the influence of the packing of and interactions between ions in the solid state on these matters remains relatively obscure. Earlier the presence of a relatively flat energy surface for  $\text{Sn}_9^{4-}$  between the  $C_{4v}$  and  $D_{3h}$  extremes and therefore a possible fluxional behavior was suggested based on some MO calculations. However, the further distinctions provided by the present two  $\text{Ge}_9$  examples suggest that the stability differences between the two configurations is subtle but perhaps real.

The supposition that the six negative charges should be proportioned  $\text{Ge}_9^{2-}$  (1) and  $\text{Ge}_9^{4-}$  (2) according to their respective geometry similarities to  $\text{B}_9\text{H}_9^{2-}$  and  $\text{Sn}_9^{4-}$  is also supported by SCF-MO-CNDO<sup>28</sup> calculations of the sort recently published for  $\text{Sn}_9^{4-}$  in various configurations.<sup>2</sup> The charge distribution assigned above corresponds to a total atomization energy for both ions of 100.5 eV, while the inverse yields 99.5 eV, or 1.0 eV less. The idealized geometries  $\text{Ge}_9^{2-}$  ( $D_{3h}$ ) and  $\text{Ge}_9^{4-}$  ( $C_{4v}$ ) yield the same energy results as the observed configurations while the alternate assignment is the poorest, 99.4 eV. The last is less precise, however, because of the lack of a good basis for estimating distances in the unknown ions.

The 1-eV energy distinction confirming the previous charge assignment comes substantially entirely from the dependence of  $\text{Ge}_9^{2-}$  atomization energy on configuration. The reason for the appreciable distortion of  $\text{Ge}_9^{2-}$  from the ideal  $D_{3h}$  must be rather subtle, a calculated 0.04-eV loss in energy probably being negligible within the precision of the calculations. Development of a small dipole moment in the direction of its nearest neighbor crypt- $\text{K}^+$  ion (1) on distortion seems like a thoroughly plausible source of stabilization in a salt where the anion has a modest polarizability. On the other hand, the electronic stability-configuration question with  $\text{Ge}_9^{4-}$  is less clear as all four configurations ( $C_{4v}$ , cluster 1 and 2,  $D_{3h}$ ) have atomization energies within  $\pm 0.06$  eV of the 44.55-eV value computed for the observed ion. However, the ideal and observed ( $\sim C_{4v}$ ) configurations for  $\text{Ge}_9^{4-}$  both have sizable calculated dipole moments, 1.9 D by these crude approximations, in contrast to the small or zero values at the other extreme. The corresponding value for  $\text{Sn}_9^{4-}$  is comparable, a good justification for its predicted reactivity.<sup>2</sup>

The earlier conclusion that a fluxional behavior was possible for  $\text{Sn}_9^{4-}$  based on the fact that the  $D_{3h}$  limit was only 0.5 eV less stable seems more complex in light of the present results. At first thought this difference might appear more significant considering real differences for the two  $\text{Ge}_9$  polyhedra. However, the  $D_{3h}$  calculation for  $\text{Sn}_9^{4-}$  was based on a model proportioned as is  $\text{Bi}_9^{5+}$ , with the prism height 15% greater

than the edges of its triangular faces, but in the present  $\text{Ge}_9^{2-}$  that difference is reduced to 10%, and in  $\text{B}_9\text{H}_9^{2-}$  the prism height is actually 3% less than the edge of the cap.<sup>25</sup> Recalculation for  $\text{Sn}_9^{4-}$  proportioned as is  $\text{Ge}_9^{2-}$  causes 60% of the 0.5-eV difference between extremes to disappear. Second, we must now face a much harder problem, the effect of a large change in dipole moment along the path in either solution or the solid state. A direct manifestation of this dipole is hard to discern in the basically close-packed structure. But sizable solvent interactions with the dipole in a  $C_{4v}$   $\text{Pb}_9^{4-}$  could well be responsible for the considerable apparent stability of the green  $\text{Pb}_9^{4-}$  in  $\text{NH}_3$  with or without crypt, in contrast with the seeming inability to generate much of this ion in en solution or to isolate it in the solid state.<sup>10</sup>

**Supplementary Material Available:** Tables of crypt- $\text{K}^+$  bond distances and angles, interionic distances, and structure factor amplitudes (25 pages). Ordering information is given on any current masthead page.

## References and Notes

- (1) Work was performed for the U.S. Energy Research and Development Administration under Contract W-7405-eng-82.
- (2) J. D. Corbett and P. A. Edwards, *J. Am. Chem. Soc.*, **99**, 3313 (1977).
- (3) E. Zintl, J. Goubeau, and W. Dullenkopf, *Z. Phys. Chem., Abt. A*, **154**, 1 (1931).
- (4) E. Zintl and A. Harder, *Z. Phys. Chem., Abt. A*, **154**, 47 (1931).
- (5) E. Zintl and W. Dullenkopf, *Z. Phys. Chem., Abt. B*, **16**, 183 (1932).
- (6) E. Zintl and H. Kaiser, *Z. Anorg. Allg. Chem.*, **211**, 113 (1933).
- (7) H. Schäfer, B. Eisenmann, and W. Müller, *Angew. Chem.*, **12**, 9 (1973).
- (8) 4,7,13,16,21,24-Hexaoxa-1,10-diazobicyclo[8.8.8]hexacosane,  $\text{N}(\text{C}_2\text{H}_4\text{OC}_2\text{H}_4\text{OC}_2\text{H}_4)_3\text{N}$ : J. M. Lehn and J. P. Sauvage, *J. Am. Chem. Soc.*, **97**, 6700 (1975).
- (9) J. D. Corbett and P. A. Edwards, *J. Chem. Soc., Chem. Commun.*, 984 (1975).
- (10) P. A. Edwards and J. D. Corbett, *Inorg. Chem.*, **16**, 903 (1977).
- (11) J. D. Corbett, D. G. Adolphson, D. J. Merryman, P. A. Edwards, and F. J. Armatos, *J. Am. Chem. Soc.*, **97**, 6267 (1975).
- (12) D. G. Adolphson, J. D. Corbett, and D. J. Merryman, *J. Am. Chem. Soc.*, **98**, 7234 (1976).
- (13) A. Cisar and J. D. Corbett, *Inorg. Chem.*, **16**, 632 (1977).
- (14) A. Cisar and J. D. Corbett, *Inorg. Chem.*, **16**, 2482 (1977).
- (15) L. Diehl, K. Khodadadeh, D. Kummer, and J. Strähle, *Chem. Ber.*, **109**, 3404 (1976).
- (16) J. D. Corbett and C. H. E. Belin, unpublished research.
- (17) R. A. Jacobson, *J. Appl. Crystallogr.*, **9**, 115 (1976).
- (18) D. G. Adolphson and J. D. Corbett, *Inorg. Chem.*, **15**, 1820 (1976).
- (19) P. Main, M. M. Woolfson, and G. Germain, "MULTAN, a Computer Program for the Automatic Solution of Crystal Structures", University of York Printing Unit, York, U.K., 1971.
- (20) D. Moras, B. Metz, and R. Weiss, *Acta Crystallogr., Sect. B*, **29**, 3, 383 (1973).
- (21) L. J. Guggenberger and E. L. Muetterties, *J. Am. Chem. Soc.*, **98**, 7221 (1976).
- (22) E. L. Muetterties and C. M. Wright, *Q. Rev., Chem. Soc.*, **21**, 161 (1967).
- (23) R. M. Friedman and J. D. Corbett, *Inorg. Chem.*, **12**, 1134 (1973).
- (24) A. Hershaft and J. D. Corbett, *Inorg. Chem.*, **2**, 979 (1963).
- (25) L. J. Guggenberger, *Inorg. Chem.*, **7**, 2260 (1968).
- (26) R. M. Friedman and J. D. Corbett, *Inorg. Chim. Acta*, **7**, 525 (1973).
- (27) J. D. Corbett, *Inorg. Chem.*, **7**, 198 (1968).
- (28) J. M. Sichel and M. A. Whitehead, *Theor. Chim. Acta*, **11**, 220, 239 (1968).